Nuclear Multifragmentation And The Onset of Radial Flow: A Study of Au + Au Collisions Between 40 and 100 MeV/A

F.Lavaud[2], E.Plagnol[2], G.Auger[1], Ch.O.Bacri[2], M.L.Begemann-Blaich[6], N.Bellaize[3], R.Bittiger[6], F.Bocage[3], B.Borderie[2], R.Bougault[3], B.Bouriquet[1], Ph.Buchet[4], J.L.Charvet[4], A.Chbihi[1], R.Dayras[4], D.Doré[4], D.Durand[3], J.D.Frankland[1], E.Galichet[5], D.Gourio[6], D.Guinet[5], S.Hudan[1], B.Hurst[3], H.Orth[6], P.Lautesse[5], J.L.Laville[1], C.Leduc[5], A.LeFevre[6], J.Lukasik[6,9], R.Legrain[4], O.Lopez[3], U.Lynen[6], W.F.J.Müller[6], L.Nalpas[4], E.Rosato[7], A.Saija[6], C.Sfienti[6], C.Schwarz[6], J.C.Steckmeyer[3], G.Tabacaru[1], B.Tamain[3], W.Trautmann[6], A.Trzcinski[8], K.Turzó[6], E.Vient[3], M.Vigilante[7], C.Volant[4], B.Zwieglinski[8].

(INDRA and ALADIN collaborations)

[1] *GANIL, CEA et IN2P3-CNRS, B.P. 55027, F-14076 Caen, France.*
[2] *Institut de Physique Nucléaire, IN2P3-CNRS et Université, F-91406 Orsay, France.*
[3] *LPC, IN2P3-CNRS, ISMRA et Université, F-14050 Caen, France.*
[4] *DAPNIA/SPhN, CEA/Saclay, F-91191 Gif sur Yvette, France.*
[5] *Institut de Physique Nucléaire, IN2P3-CNRS et Université, F-69622 Villeurbanne, France.*
[6] *Gesellschaft für Schwerionenforschung mbH (GSI), D-64291 Darmstadt, Germany*
[7] *Dipartimento di Scienze Fisiche e Sezione INFN, Universita di Napoli "Federico II", I-80126 Napoli, Italy.*
[8] *Soltan Institute for Nuclear Studies, Pl-00681 Warsaw, Poland.*
[9] *Institute of Nuclear Physics, Pl-31342 Krakow, Poland.*

Abstract. The influence of radial flow on nuclear multifragmentation is studied using Au+Au central collisions for incident energies between 40 and 100 MeV/A. Central collisions are selected via an impact parameter estimator defined by the transverse energy of light charged particles. At all energies, the fragment size distributions are studied using the Statistical Multifragmentation Model (SMM) in order to extract thermal excitation energies. The excess kinetic energies are analyzed via the hypothesis of a radial, self-similar, but non-isotropic flow. At the lowest energy, this flow is small with respect to the thermal energy whereas, at 100MeV/A thermal and radial energies are of the same order. The nature and origin of the radial flow is discussed. A comparison with the predictions of the Quantum Molecular Dynamics code is presented.

INTRODUCTION

Nuclear multifragmentation, i.e. the observation of a *many fragment* reaction channel is one of the most interesting aspects of heavy ion collisions in the Fermi energy domain (25-100 MeV/A incident energies for symmetric systems). Many facets of this process (moments of the fragment size distribution, kinetic energies,…) have led to associate it to the physics of phase transitions. The observation of a *multifragment configuration* would correspond to a state of matter intermediate between a nuclear liquid (the nucleus close to its ground state) and a nuclear vapor (an assembly of nucleons and light fragments at high temperature). The study of nuclear multifragmentation would be one of the rare possibilities of studying, *microscopically*, a phase transition in a finite size fluid.

Assuming that thermal and chemical equilibrium has been reached at some point in time during the nuclear reaction, the final products of the collision are usually compared to the predictions of statistical models which consider a hot gas of non-interacting fragments. In the nuclear physics community, these comparisons are done within the framework of the SMM[1] or MMMC[2] models.

This type of comparison generally leads to the conclusion that the final characteristics of the products (fragment sizes and kinetic energies) are determined at a low-density *freeze-out* point at which the short range nuclear force ceases to act between the fragments. It is not clear however, whether these characteristics are uniquely determined at this freeze-out point or to what extent the dynamical evolution, from the initial thermalized configuration to the freeze-out point, plays a role.

Indeed, closely associated to the process of multifragmentation has been the observation of a radial, self-similar, velocity flow[6,7]. This flow corresponds to an excess kinetic energy which fragments are seen to have when compared to the predicted thermal+Coulomb energies at the freeze-out point. The origin of this flow is not well understood and several suggestions have been put forward: transparency effects, compression-decompression,… [18]

In order to study in more detail these questions, data of high quality and precision are necessary. To this end, the Au+Au collisions were studied for beam energies in the range between 40 and 150 MeV/A. These reactions were studied at the SIS accelerator facility at GSI (Darmstadt, Germany) with the INDRA 4π detector. A detailed description of this detector can be found in J.Pouthas et al. [10].The work described in this contribution constitutes the Ph.D. thesis of F.Lavaud. A more detailed description will be given in a forthcoming publication.

THE SELECTION OF CENTRAL EVENTS

Although multifragmentation is observed for non central collisions, it is for the smallest impact parameters that these processes are more clearly identified. In order to select these central collisions, we use an impact parameter estimator[21] that is related to the total transverse energy ($E_{transZ12}$) of light charged particles (LCP, Z≤ 2) :

$$b\left(E_{trans12}\right) = b_{\max}\frac{\sqrt{\int_{E_{trans12}}^{E_{trans12\_max}}\sigma\left(E_{trans12}\right)}}{\sqrt{\int_{E_{trans12\_min}}^{E_{trans12\_max}}\sigma\left(E_{trans12}\right)}} \qquad \text{eq.1.}$$

where b_{max} is determined from the total detected reaction cross-section. In the present study, this reaction cross section corresponds to events with a minimum multiplicity of 4 charged particles.

The normalized cumulated cross-section as given by equation 1, shows a quasi-linear behavior. It is remarkably invariant with respect to the incident energy when the value of $E_{transZ12\_max}$ is normalized with respect to the total available center of mass energy.

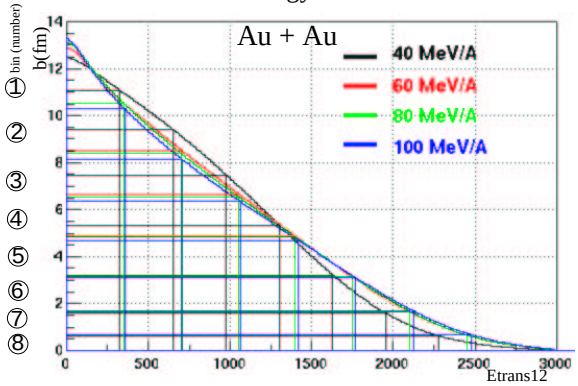

Figure 1. Correlation between the impact parameter b and $E_{transZ12}$ in the case of Au+Au collisions at incident energies of 40, 60, 80 and 100 MeV/A.

Figure 1. shows the correlation between the impact parameter estimator b and $E_{transZ12}$ for the different incident energies studied. A similar type of correlation has also been observed for other systems[11] and J.Lukasik et al.[12] will give, in these proceedings, other examples. The cross section is then divided into 8 bins, with bin 8 representing the 5% smallest values of the impact parameter estimator. In this study, bins 7 and 8 will represent the "central collisions" studied in detail below. The sum of these two bins represent a cross section of the order of 100 mb and a maximum impact parameter close to 2.0 fm. It has been checked that the conclusions of this study do not depend on this particular impact parameter estimator. Other types of selection, based on *global event variables* lead to similar conclusions

STATISTICAL ANALYSIS AND THERMAL ENERGIES

Selecting bins 7 and 8 (c.f. figure 1.), we have made the *a-priori* hypothesis that they could be analyzed within the statistical model. The SMM model has been used throughout all this study but very similar results were obtained with the MMMC code. The system is defined by its size (Z_0, A_0), its density (ρ) at freeze-out and its "thermal" excitation energy E_0. Because of pre-equilibrium effects, Z_0, A_0 and E_0 are considered to be adjustable parameters

and will not correspond to the total available charge, mass and energy. In this study ρ has been fixed at 1/3 of normal nuclear density (ρ_0). Figure 2. shows the fragment size distributions measured at various incident energies and the fits obtained with the statistical model. The data correspond to those products detected in the center of mass angles between 0° and 90° where the INDRA efficiency is highest. The size, density and thermal excitation energies used in the calculations are given in the first columns of table 1 for the different incident energies. Figure 3. shows, at 100 MeV/A, that these fragment size distributions are independent of the angle of observation, consistent with the statistical hypothesis. This isotropy has been observed at all energies.

Table 1. SMM parameters from a fit to the kinetic energies of fragments for a deformed freeze-out configuration.

Incident Energy (MeV/A)	Z_0	A_0	E_0 (MeV/A)	density	Deformation	Radial flow (MeV/A)	Thermalized Energy
40	142	355	6.0	$\rho_0/3.$	2.1	2.0	73%
60	125	312	7.8	$\rho_0/3.$	2.0	4.5	65%
80	110	275	8.7	$\rho_0/3.$	1.7	8.0	58%
100	95	237	9.1	$\rho_0/3.$	1.5	9.0	43%

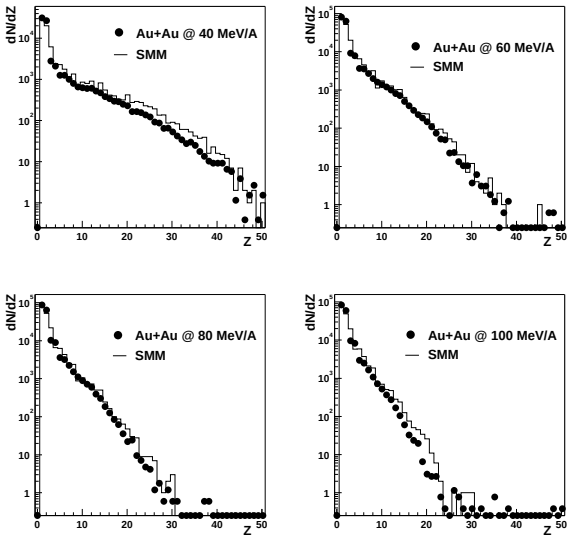

FIGURE 2. Comparison of the fragment size distribution obtained at various incident energies with the predictions of the SMM code. The data correspond to products detected in the center of mass angles between 0° and 90° in central collisions (bin 7 and 8, see text). The size and thermal excitation energies used in the calculations are given in table 1.

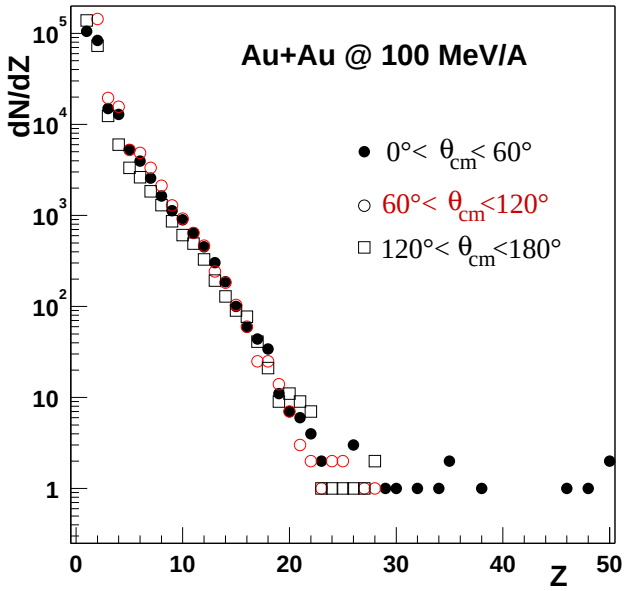

FIGURE 3. Comparison of the fragment size distribution obtained for central collisions (bin 7 and 8, see text) at an incident energy of 100 MeV/A at different angles in the center of mass.

RADIAL FLOW AND DEFORMATION

Although the distributions of fragments are observed to be isotropic (Fig. 3.), the study of the kinetic energies are seen to deviate from what would be expected for a standard statistical emission. The kinetic energies are observed to be, at the higher incident energies, much larger than predicted by the statistical model which assumes a thermal (Maxwellian spectrum) part and a Coulomb repulsion calculated for the corresponding freeze-out density.

Figure 4. shows the kinetic energies, as a function of the charge Z of the detected ion for the different incident energies and for different angular range. In order to reproduce these data, and following the suggestion by A.Le Fevre et al.[13] and B.Bouriquet[15] et al., two supplementary assumptions have been made: i) a deformed, ellipsoidal, shape for the freeze-out volume and ii) a self-similar radial flow. Because of the elliptic geometry of the freeze-out configuration, the resulting kinetic energy distributions are non-isotropic, i.e. the mean kinetic energies are larger at 0° than at 90°. The parameters obtained, via the fitting procedure, are given in the last 3 columns of table 1. The partition functions are, in this calculation, not affected by the characteristics of the freeze-out geometry. The *deformation* parameter given in table 1 is the ratio of the longest axis (aligned with the beam direction) to the

length of the axis perpendicular to it (axial symmetry along the beam axis is assumed). Figures 4 and 5 compare the result of these calculations to the measured data.

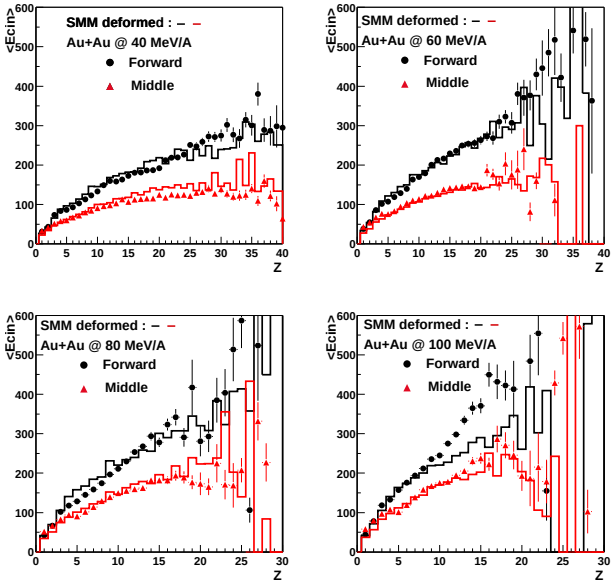

FIGURE 4. Comparison of the kinetic energy distributions (bin 7 and 8, see text) as a function of the charge of the detected ions obtained at various incident energies and for two angular ranges (forward: $0°\leq\theta_{cm}\leq60°$, middle: $60°\leq\theta_{cm}\leq120°$). The histograms give the predictions of the statistical model SMM with an ellipsoidal freeze-out volume and a self-similar radial flow. Parameters used in the calculations are given in table 1.

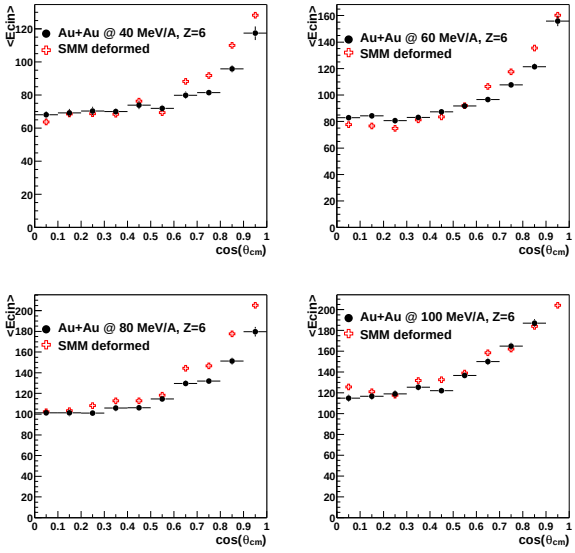

FIGURE 5. Evolution of the mean kinetic energies for Z=5 as a function of the center of mass angle for the different incident energies. The crosses give the predictions of the statistical model SMM with an ellipsoidal freeze-out volume and a self-similar radial flow. Parameters used in the calculations are given in table 1. The data correspond to bin 7 and 8, see text.

Figure 6 and 7 show the fits obtained for the spectra of some individual kinetic energy distributions.

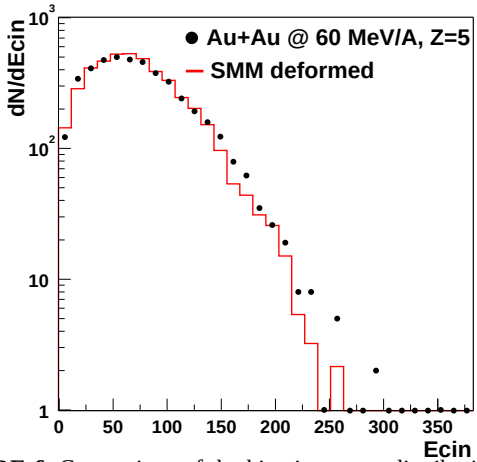

FIGURE 6. Comparison of the kinetic energy distributions of Z=5 ions observed at Elab=100 MeV/A with the predictions of a deformed SMM calculation. Parameters used in the calculation are given in table 1. The data correspond to bin 7 and 8, see text.

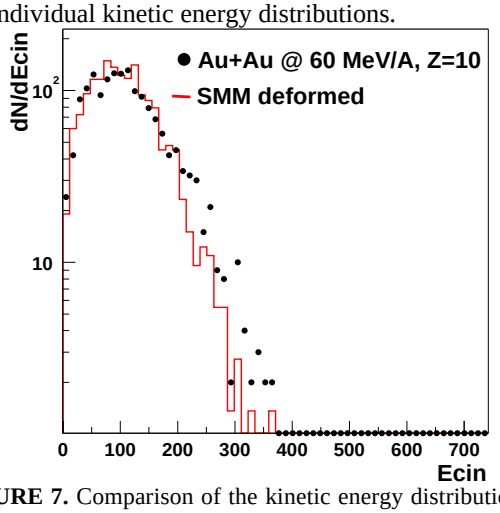

FIGURE 7. Comparison of the kinetic energy distributions of Z=10 ions observed at Elab=100 MeV/A with the predictions of a deformed SMM calculation. Parameters used in the calculation are given in table 1. The data correspond to bin 7 and 8, see text.

DISCUSSION

The parameters given in table 1 and which have been obtained from a fit to the data using a deformed freeze-out geometry associated with a self-similar radial flow reveal certain interesting features. As a function of beam energy, the size of the thermalized source decreases strongly from almost the whole system to close to half of it (two Au nuclei correspond to Z_{tot}=158, A_{tot}=394). This implies that pre-equilibrium effects increase strongly with incident energy and that many LCP, and neutrons, escape the bulk of the matter before thermalization is achieved. The second feature is that although the available center of mass energy more than doubles (from 10 MeV/A to 25 MeV/A), the extracted thermal energies increase only by 50%. A large part of the remaining energy goes into radial flow, which evolves from 2 MeV/A (1/3 of E_0) to 9 MeV/A (equal to E_0). Altogether, the energy fraction *converted* into the thermalized source represents 73% at 40 MeV/A and 43% at 100 MeV/A (see last column of table 1). An inspection of the different figures shows the remarkable quality of the fits obtained. Although a number of parameters are available to achieve this, the quality of the fits appear to give some credit to the underlying physical picture.

The observation of radial flow associated to a deformed freeze-out suggests a number of remarks. It is first necessary to note that the flow energies quoted are analysis dependent. This is due to the fact that a given constant density ($\rho_0/3$) has been assumed. The energy spectra, such as shown in figures 6 and 7, reflect the sum of i) a thermal energy (assumed to be of Maxwellian shape with a temperature T), ii) a potential energy due to the Coulomb repulsion and iii) the extracted radial flow. However, the last two contributions cannot be distinguished if the flow is assumed to be self-similar. This radial flow value could thus be lowered by increasing the freeze-out density. The observation of an increasing radial flow could thus reflect the increase of the "maximum density" that the system reaches during its evolution. This, in turn, leads to the question of what region in T,ρ space the system is sensing and which region determines its final structure, i.e. the observed fragment size distribution. X.Campi, H.Krivine and N.Sator[3] have addressed this problem for a system of uncharged-classical particles. They conclude that the fragment size distribution is mainly determined by the total energy of the system and not by its specific location in T,ρ space. Work along these lines is in progress for high density *charged* systems, showing that the initial (long range) Coulomb potential energy is indeed transformed into kinetic energy at infinity[19] and not thermalized. The question of the temperature(s) that are relevant for the system is still not clearly understood and will be studied in this framework.

Another point that can be discussed is the meaning and values of the deformation parameter. The origin of this deformation is unclear. It could result from the way that the system reaches its maximum density point, a *memory* of the incoming direction could well be preserved during the following expansion. It could also originate from a partial transparency of the incoming ions. The fact that this deformation decreases with increasing beam energy could indicate that the nucleon-nucleon cross-section becomes more efficient and hence the transparency less apparent.

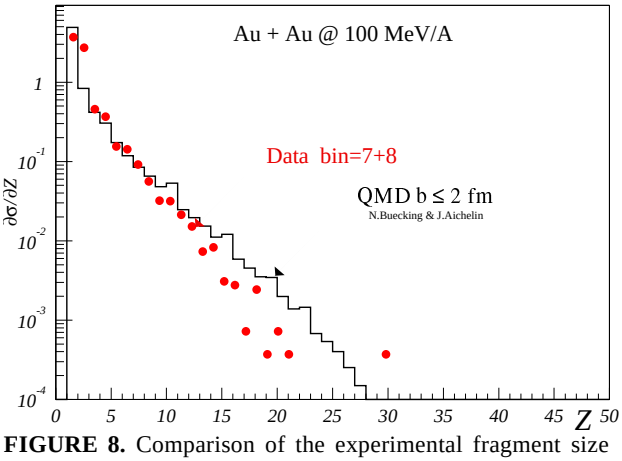

FIGURE 8. Comparison of the experimental fragment size distributions obtained for central collisions (bins 7 and 8, see text) with the predictions of the QMD code.

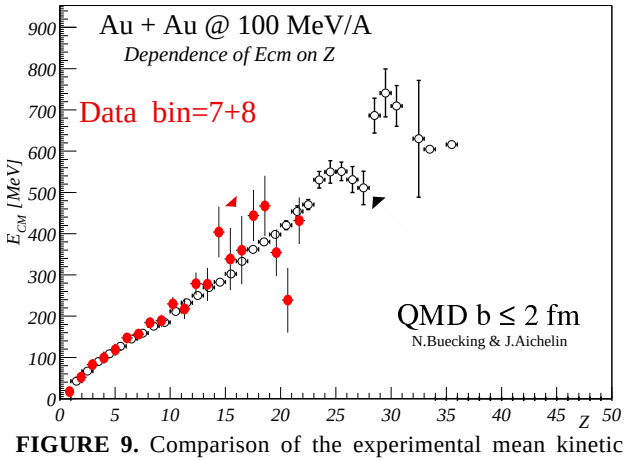

FIGURE 9. Comparison of the experimental mean kinetic energy as a function of the charge of the fragment obtained for central collisions (bins 7 and 8, see text) with the predictions of the QMD code.

A number of the questions raised above should be answered by the study of these collisions with a dynamical model. The QMD model[20] has often been used in this respect. R.Neubauer and J.Aichelin[16] have extensively

studied the Xe+Sn collisions (INDRA data). N.Buecking and J.Aichelin[17] have applied this model to Au+Au central collisions (b≤2fm) at 100 MeV/A beam energy.

Figure 8 and 9 compare the experimental data to the results of this code. Both the fragment size distribution and the average kinetic energies (as a function of the fragment charge) are very well reproduced. This is also true for other variables such as the width of the rapidity distribution for individual fragments. A more detailed analysis of the comparison between data and code results is in progress. At this moment, the authors of this study have observed that the fragments detected at mid-rapidity for central collisions reflect a mixing of projectile and target nucleons. If this is verified, the claim that the observed multifragmentation results from the decay of a thermalized source would be partially substantiated by this code. This would open up new and interesting ways to study the *dynamics* of the nuclear liquid-gas phase transition.

ACKNOWLEDGMENTS

The authors would like to express their tanks to the crew of the SIS accelerator staff for beams of excellent quality and to INDRA and GSI Cave B technical support without which this experiment would not have been possible.

REFERENCES

1. J.P.Bondorf et al. Phys. Rep. **257** (1995) 133
   A.S.Botvina, A.S.Iljinov, I.N.Mishustin, J.P.Bondorf, R.Donangelo and K.Sneppen, Nucl. Phys. **A475** (1987) 663-686.
2. D.H.E.Gross, Nucl. Phys. **A428** (1984) 313
3. X.Campi, H.Krivine and N.Sator, Nucl. Phys. A**681** (2001) 458c
   N.Sator Ph.D Thesis, Université Paris XI, Orsay 2000, unpublished.
4. E.Plagnol and F.Lavaud, In Proc. of the XXXIX Int. Winter Meet. on Nucl. Phys., ed. by I.Iori and A.Moroni,, 2001
5. F.Lavaud , E.Plagnol et al. In Proc. of the XXXIX Int. Winter Meet. on Nucl. Phys., ed. by I.Iori and A.Moroni,, 2001
6. W.Reisdorf and H.G.Ritter, Annu. Rev. Nucl. Part. **47** (1997) 663.
7. S.Salou Phd dissertation, Ganil, Univ Caen, 1997.
8. D'Agostino et al., Phys. Lett. **B371** (1996)175.
9. W.C.Hsi et al., Phys. Rev. Lett. **73** (1994)3367.
10. J.Pouthas and the INDRA coll., NIM **A357** (1995) 418.
11. J.Lukasik, E.Plagnol and the INDRA coll., Phys. Rev. **C55** (1997) 1906.
12. J.Lukasik, in these proceedings.
13. A.Le Fevre, M.Ploszajczak and V.D.Toneev, Phys. Rev. **C60** 051602 (1999).
14. N.Marie et al., Phys. Lett. **B391** (1997) 15.
15. B.Bouriquet et al. In Proc. of the XXXIX Int. Winter Meet. on Nucl. Phys., ed. by I.Iori and A.Moroni,, 2001.
16. R.Neubauer and J.Aichelin Nucl. Phys. A**683** (2001) 605
17. N.Buecking and J.Aichelin, private communication.
18. C.Hartnack and J.Aichelin, Phys. Lett. B 506(2001)261
19. E.Plagnol and F.Lavaud, work in progress.
20. J.Aichelin, Phys. Rep. 202(1991)233
21. C.Cavata et al. Phys. Rev. C42 (1990)1760